Technische Universität München
Lehrstuhl für Nachrichtentechnik
Prof. Dr. sc. techn. Gerhard Kramer

Bachelor's Thesis

Communication over unknown channel

Vorgelegt von:
Kevin Li

München, January 2018

Betreut von:
Marcin Pikus

Bachelor's Thesis am
Lehrstuhl für Nachrichtentechnik (LNT)
der Technischen Universität München (TUM)
Titel : Communication over unknown channel
Autor : Kevin Li

Kevin Li
Am Römerbrunnen 6
85586 Poing
kev.li1010@gmail.com

Ich versichere hiermit wahrheitsgemäß, die Arbeit bis auf die dem Aufgabensteller bereits bekannte Hilfe selbständig angefertigt, alle benutzten Hilfsmittel vollständig und genau angegeben und alles kenntlich gemacht zu haben, was aus Arbeiten anderer unverändert oder mit Abänderung entnommen wurde.

München, 22.01.2018

Ort, Datum (Kevin Li)

Contents

List of Figures

List of Tables

1. Introduction

1.1. Intro

With the ever growing market of mobile devices and the slow approach of next generation of wireless communication in form of 5G an utmost importance and interest is set on wireless communication. While in itself LTE or 4G can be explained shortly for a layman to understand there are many techniques and difficulties behind it before reaching a feasible wireless transmission. Most recently seen in the development of the 5G network with its unofficial launch date as standard communication system in 2020. (!!cite!!) In this thesis we will discuss the difficulties of transmission of data in unknown channel. A functioning channel consisting of transmitter and receiver will be built and different channel settings will be tested. Different solutions will be given to increase transmission efficiency and error rates of the system.

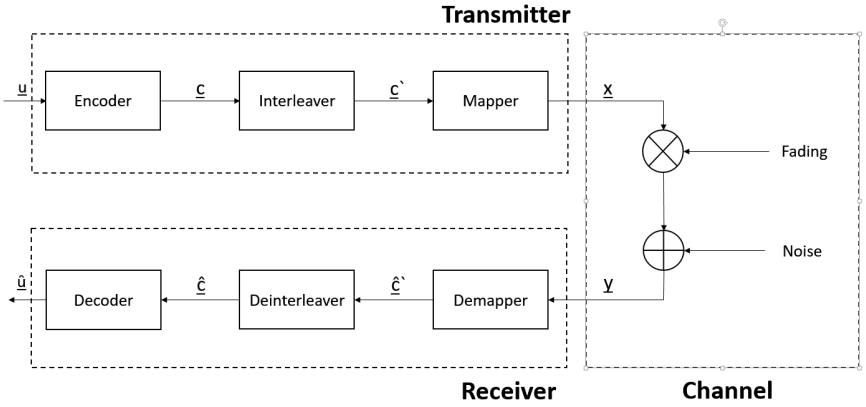

Figure 1.1.: PDF $p_N(N)$ of the number N of times that the head side is up.

2. Communication Chain

First, the communication chain for simulations is introduced in Figure 2.1. The link is built up of three main blocks: The transmitter, channel and receiver. Transmitter in turn contains the encoder, interleaver and mapper. We start with feeding a random generated bit stream, representing a message, $\underline{u}$ into the encoder. The resulting encoded code word $\underline{c}$ is next processed in the interleaver producing the shuffled code word $\underline{c}$'. The mapper can now modulate $\underline{c}$' into the desired modulation scheme with the symbol array $\underline{x}$. In the channel various kind of noises and fading can be added to the modulated signal, e.g., additive white gaussian noise (AWGN). In the later half the receiver, consisting of the counterparts build in the transmitter, will first demap the signal $\underline{y}$ to the estimated code word $\underline{\hat{c}}$. After de-interleaving and decoding the transmitted symbol an estimate $\underline{\hat{u}}$ is determined. In the simulation we will compare the decoded message $\underline{\hat{u}}$ with the initially created input message $\underline{u}$ to calculate the error rate in the system.

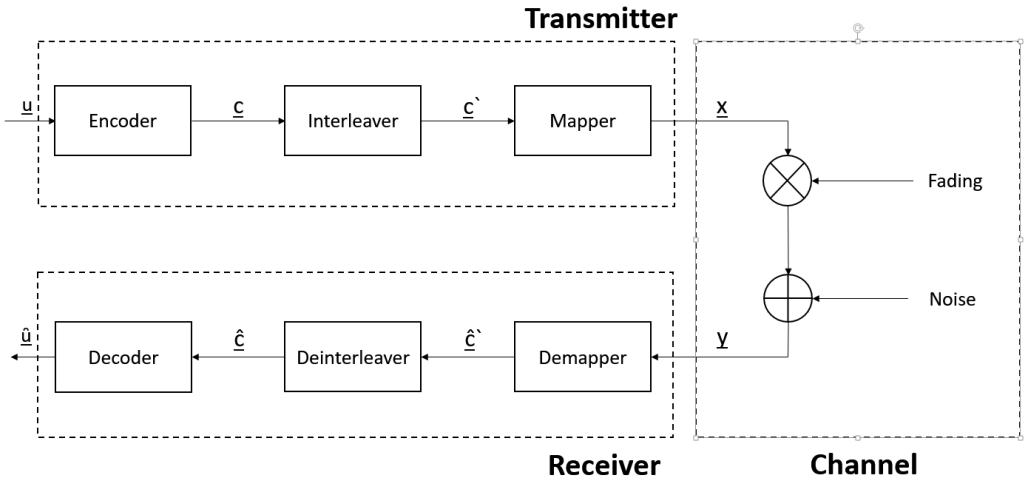

Figure 2.1.: Communication chain for simulation

2.1. Encoder/Decoder

There are many ways to make the transmission more stable and less error prone. A major role in this protection plays the encoder and its counterpart the decoder. Encoder/decoder come in many different forms and shapes, e.g., as pre-built circuits in systems but more commonly today as software coder. They reach from simple linear block codes to more complex convolutional coding to the latest turbo codes. It is also important to note, that one coder working well in AWGN channel will often not have the same performance in a fading channel. (cite)
A further look will be taken into low density parity check (LDPC) codes, in particular the WiMax code. !!citation!!. While LDPC was mainly ignored in the past, since the 1999's the introduction of turbo codes and a sharp increase in computing power helped the recognition of these forms of channel coding.
LDPC codes are linear block codes with a particular structure for their parity check matrix **H**. In the case of LDPC-codes **H** has only a small amount of nonzero entries, which means that there is a low density in the parity check matrix. Another important difference in LDPC to turbo codes is the complexity of encoding and decoding. While turbo codes have low complexity in encoding they have high complexity in decoding. The total opposite can be said about LDPC with high complexity in encoding and low complexity in decoding.
WiMax IEEE 802.16e is a standard code model used in small and medium distances in urban areas, which fits the simulations quite well. It should be noted, that for WiMax there are predefined code lengths and code rates and encoding classes. Code lengths can range from 576 bits up to 2034 bits. Code rates !!footnote!! are divided into four rates[1]: 1/2, 2/3, 3/4, 5/6 and the coding class used is only A, class B will be ignored.

[1] $R = \frac{\text{Number of relevent data bits}}{\text{Number of overall data bits}}$

2.2. Bit interleaver/De-interleaver

While the above mentioned LDPC codes (Chapter (2.1)) work really well for an AWGN channel this is not always the case in a fading channel. Therefore another important block must be included in the channel. To guarantee a stable performance the method of interleaving will be introduced. Interleaving will handle a major problem in fading channels, namely the appearence of burst errors caused by deep fading over a set time. LDPC coding suffers from loss of performance trying to correct these burst errors, deteriorating even more with the increase of the burst error length. With the interleaver the code word will be shuffled into a new random Gaussian distributed code word, which will be passed through the channel. At the receiver a restoration of the shuffled code word back into its initial state will take place.

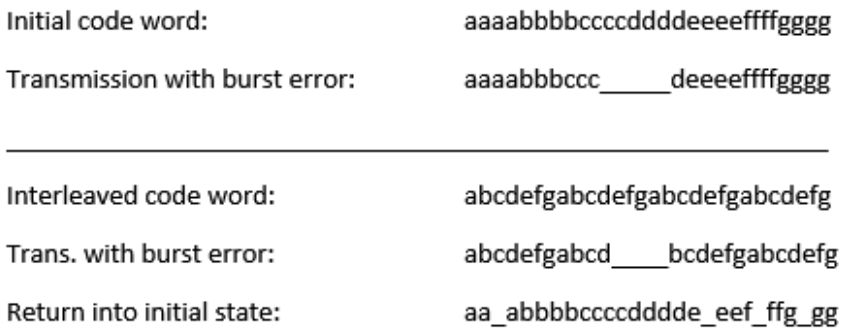

Figure 2.2.: Example for interleaving

As clearly seen in Figure 2.2 the interleaver will not remove any errors but will prevent or at least mitigate the presence of burst errors. The LDPC decoder can correct single errors again. There are two main methods of interleaving today: symbol-interleaved coded modulation (SICM) will interleave the symbols after the modulator while bit-interleaved coded modulation (BICM) will interleave the single bits before the modulator block. BICM will be used in this thesis for having a more dominant position in practical communication systems. !!cite!!

2.3. Mapper/Demapper

In this block the mapper, also called the modulator, makes it possible to assign the code word a specific symbol. Group of bits are taken from the bit stream to combine them to specific constellation points. The symbols are located in a real/imaginary plane, also called Inphase/Quadrature planes (I/Q-planes). With the distance from the nullpoint of the axis giving us the magnitude of the signal and the angle to the real axis the phase shift.

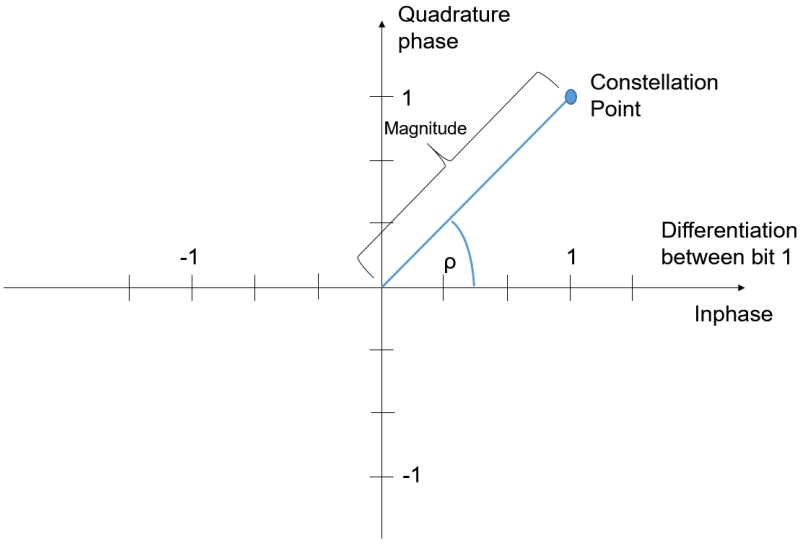

Figure 2.3.: Example for constellation point with amplitude and phase shift angle (ϕ)

There are many forms of modulation schemes, with the most common ones being M-phase shift keying (PSK), M-frequency shift keying (FKS), M-amplitude modulation (AM) and M-quadrature amplitude modulation (QAM). For the simulation, a further look will be taken at quadrature phase shift keying (QPSK), 16-QAM and 64-QAM, which are all depicted in Figure 2.4.
With QPSK the symbols all share the same amplitude and only differ in their respective phase angle. To each symbol we can assign $log2(M)$ bits, with M being the number of symbols in the scheme. Therefore, for QPSK the number of bits per symbol amount to 2.
For QAM, signals which differ in their phase shift and also their amplitude, will be sent. For 16-QAM a maximum of 4 bits per symbols and for 64-QAM 6 bits per symbol can be achieved.

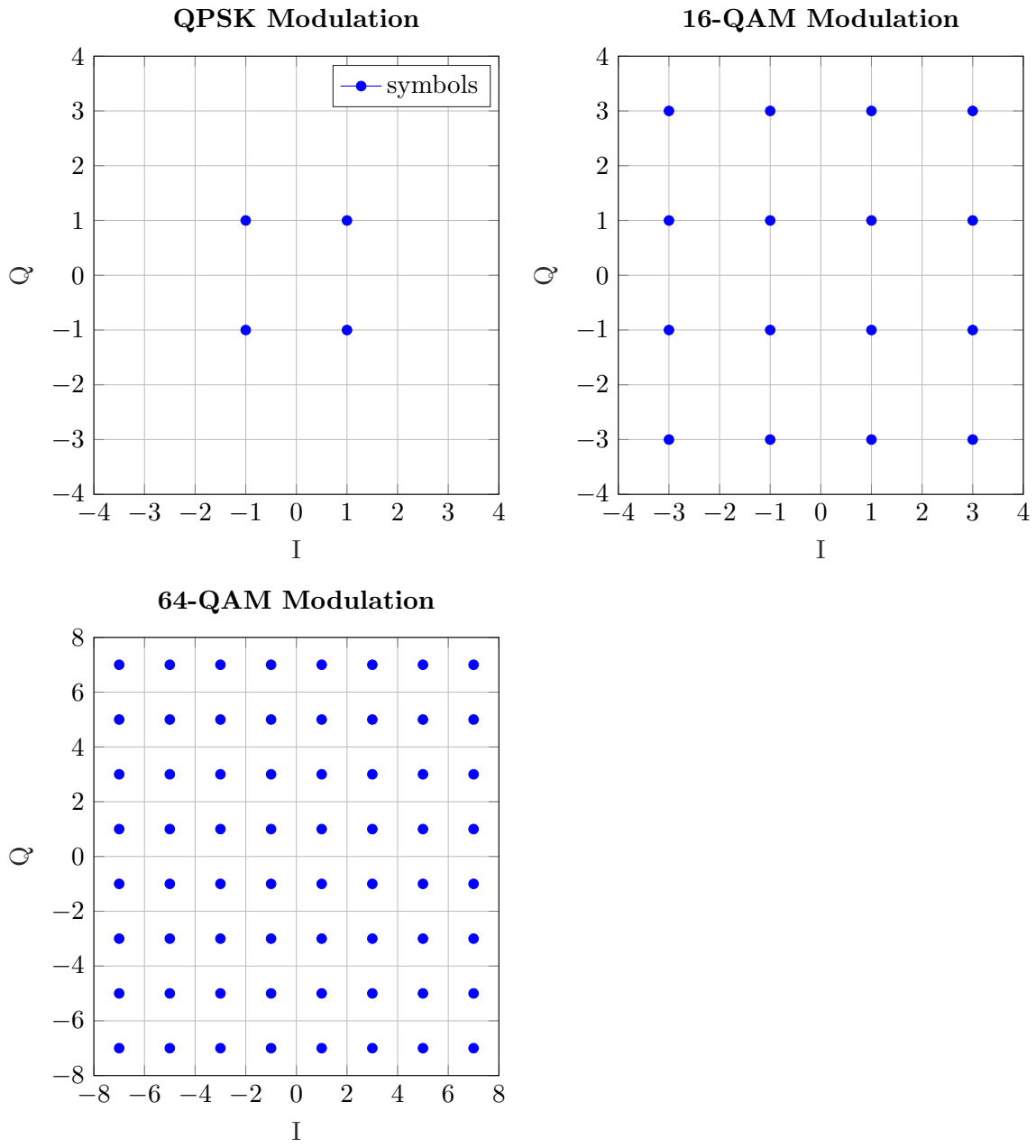

Figure 2.4.: Modulation in I/Q planes for QPSK, 16-QAM and 64-QAM

2.4. Channel

The channel can be modeled in many different ways. Various sources of noise or fading can be applied, which will relate to real world interferences. Some interferences experienced in real life transmission are, e.g., thermal noise, distance fading, doppler effect and reflection of signals. To approach those kind of interferences there are many different channel models, like the AWGN channel or Rayleigh/Rician fading. A further look in the AWGN channel and Rayleigh fading will be given. A small graphic will further illustrate the usual culprits for degradation of signal power and resulting loss in communication performance (Figure 2.5).

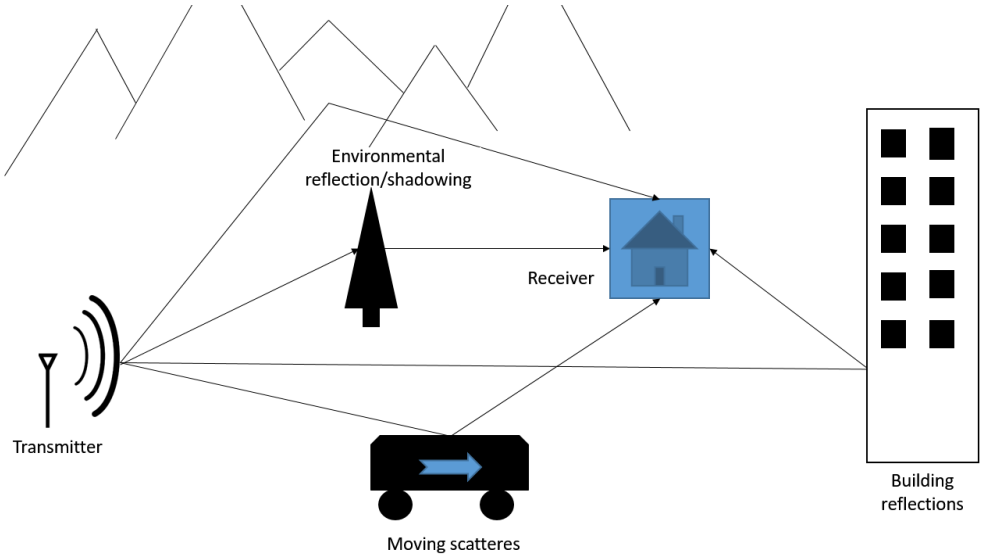

Figure 2.5.: Interferences in a normal transmission between two devices

2.4.1. AWGN Channel

The easiest kind of channel manipulation is to add random Gaussian noise to the channel, also commonly known as an AWGN channel. Like the name says we will add noise, which is a random Gaussian distribution with flat spectral density, to an existing transmitted signal. Our receiver will receive a signal like this:

$$Y = X + N, \tag{2.1}$$

with Y being the received symbols, X the send symbol and N the complex AWGN noise. This can be applied for a full transmission of messages resulting in:

$$\underline{Y} = \underline{X} + \underline{N}, \tag{2.2}$$

which can be depicted more detailed like this:

$$[Y_1, Y_2, ..., Y_n] = [X_1, X_2, ..., X_n] + [N_1, N_2, ..., N_n] \tag{2.3}$$

The probability density function is defined as follows:

$$f(y|x) = \frac{1}{\pi\sigma^2} * e^{-\frac{(y-x)^2}{\sigma^2}}, \tag{2.4}$$

with y being the acquired point,x the transmitted symbol and σ^2 the variance of the distribution. Gaussian noise, representing thermal noise and overlay with multiple users in a wireless system, is therefore used in all the simulations run in this thesis. In Figure 5.1 a depiction of the spectral power distribution of AWGN, where it can clearly be seen that it is flat and spread evenly over the whole spectrum.

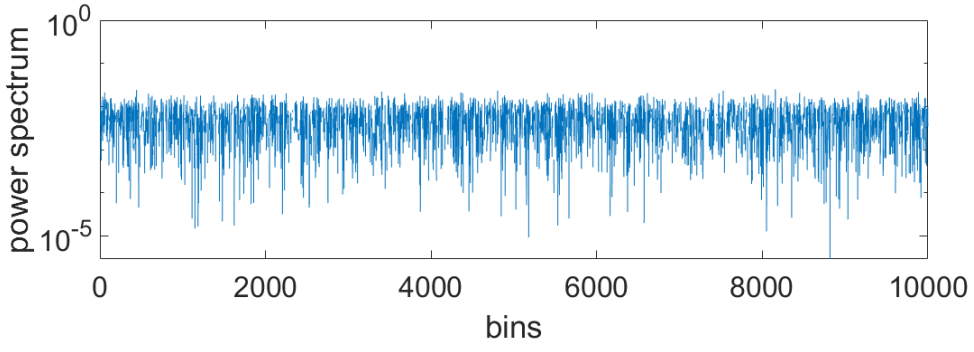

Figure 2.6.: Power spectral density in a AWGN channel

2.4.2. Rayleigh Channel

Another common channel model used in communication theory is Rayleigh fading. Rayleigh fading simulates multipath reception, which means that for a receiver antenna in a wireless link there are many reflected and scattered signals reaching it (Figure 2.5). These kind of reflections are often seen in high-density urban areas. This results in construction or destruction of signal waves. The channel will now look like this:

$$Y = H * X + N, \tag{2.5}$$

which adds the new Rayleigh fading coefficient H. !!footnote explaining H!!
As shown before in the AWGN channel the above Equation (2.5) can be expanded for a full transmission. Before that it needs to be clarified that not every symbol will be multiplied with a different fading coefficient H, but a block of symbols. This kind of transmission with Rayleigh fading is known as block fading:

$$[Y_1, Y_2, ..., Y_T] = H * [X_1, X_2, ..., X_T] + [N_1, N_2, ..., N_T], \tag{2.6}$$

with the subscript T indicating the length of the block. The block length can be chosen ranging from on single symbol up to the whole code word being one block. The PDF according to the calculations above is:

$$f(y\sigma) = \frac{1}{\sigma^2} e^{-\frac{y^2}{2\sigma^2}}, \tag{2.7}$$

The graphic (Figure 2.7) shows the power distribution over 12000 samples. Being Gaussian randomly distributed there are now these so called "deep fadings" where the power of the fading drops, which will also decrease the signal power of the received signal to drop significantly. This results in the so-called burst errors, which were mentioned in Chapter (2.2).

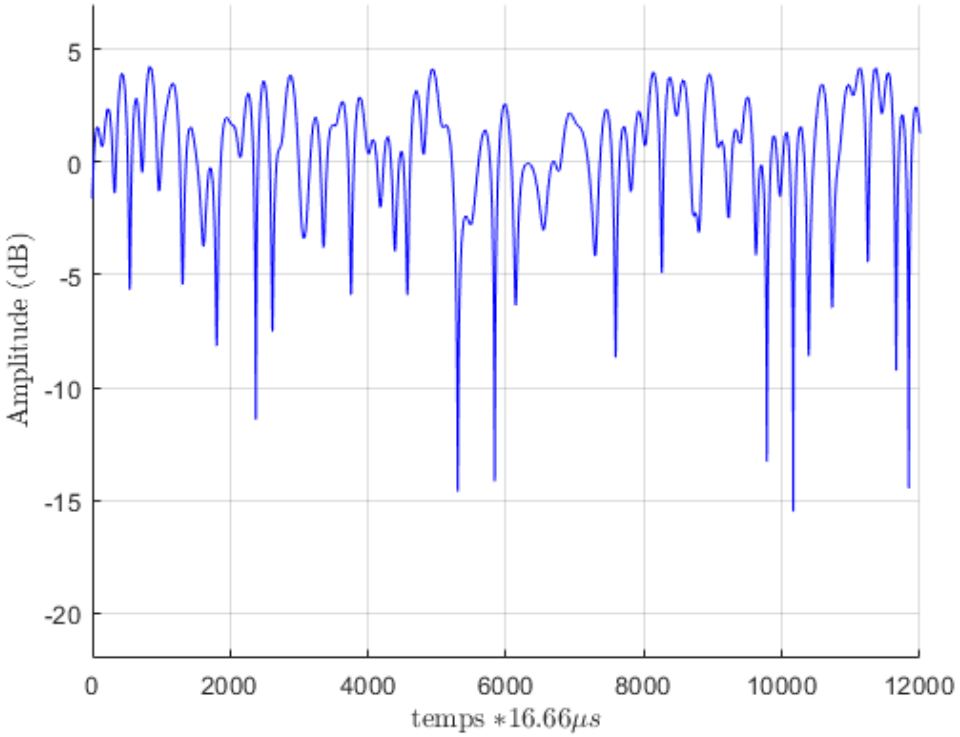

Figure 2.7.: Power spectral density in a rayleigh channel

3. Capacity in AWGN Channel

In this section we will discuss the capacity of a wireless channel with AWGN noise interfering with the transmission between transmitter and receiver.
In general capacity C can be defined as the maximum data rate R at which information can be reliably transmitted over a channel, that means the highest rate of transmission with a very low error probability rate. It is proven that any rate exceeding the maximum capacity rate of the channel will result in error rates deviating from zero (!!cite!!). In modern technology with the help of smart modulation schemes and coding methods a rate close to the capacity can be achieved. All the capacities in the following simulations will be complex and also time-discrete. While time-continuous systems are analyzed for real world applications, most systems can be converted into a time-discrete model with same capacity results. The transformation will also be shown in the following sections.

3.1. Capacity and Monte-Carlo-Simulation

For a AWGN-Channel the simple channel model already defined in Equation (2.1) will be used:

$$Y = X + N, \tag{3.1}$$

with X $\sim N(0,{\sigma_T}^2)$ and N $\sim N(0,1)$. The received signal Y will have a distribution of Y $\sim N(0,{sigma}^2{+}1)$ under the condition that X and N being independently distributed. Now the capacity as a maximum of mutual information I between X and Y will be calculated:

$$C = max(I(X;Y)), \tag{3.2}$$

with X and Y being two independent randomly normal distributed variables.
For the mutual information further calculations will lead to the differential entropy:

$$I(X;Y) = h(Y) - h(Y|X) = h(Y) - h(N), \tag{3.3}$$

with N also being independent from X.
This further simplifies to

$$h(Y) = h(X+N) = log(\pi * e^{\sigma^2+1}) \quad \text{and} \quad h(Y|X) = h(N) = log(\pi * e^1), \tag{3.4}$$

which will lead us to the final equation for the capacity in an AWGN-channel:

$$C = log(1+\sigma^2) \tag{3.5}$$

With this approach a good approximation of values for further calculations with added modulation schemes has been given. The above calculated data rate can be used as upper bound for any further capacity calculation done, this means there should be no capacity rate, especially for real world applications, exceeding this capacity rate (Equation (3.5)).

3.2. Capacity for QPSK and M-QAM

Now the capacity will be calculated for the three above mentioned modulation schemes (Chapter (2.3)). The schemes will be plotted with the capacity calculations for the AWGN channel to give us a overall comparison and overview.
Before the simulation or any calculation is done it can already be assumed how QPSK will behave for high SNR. As stated before QPSK (Chapter (2.3)) can transmit up to 2 bits per symbol, but no more without losing its reliability in transmission. So the plot will approach the 2 bit per symbol border for high SNR. The same assumption can be applied to both 16-QAM and 64-QAM. After creating a random codeword modulated with the fitting modulation scheme, noise is added to the signal, which is then received as the bit stream Y. The next step is to calculate the capacity.
Starting with the mutual information again we get:

$$I(X_Q;Y) = h(Y) - h(Y|X_Q) = h(Y) - h(N) \tag{3.6}$$

It is known that the signal is normal random distributed variable and now the differential entropy for h(Y) has to be calculated:

$$h(Y) = \int p(y) * [-log(p(y))]\text{dx} \tag{3.7}$$

Applying the Monte-Carlo-Simulation will simplify the above equation so it can be solved numerically, turning the time-continuous system into a time-discrete form. The Monte-

Carlo-Simulation will be further explained in the following chapter (Ch. 3.2.1).

$$h(Y) = \sum_{i=0}^{N}(-log(p(y_{\mathrm{i}}))) * \frac{1}{N}, \tag{3.8}$$

with p(y) being the probability of y for a normal distributed variable and N the number of iterations. Now p(y) has to be further defined as it takes in consideration the possible input and output pairs $x \in X$ and $y \in Y$. The sum over all these pairs is taken:

$$p(y) = \frac{1}{k * \pi} * \sum_{n=1}^{k}(e^{y-x_{\mathrm{n}}}), \tag{3.9}$$

with x being the constellation points and y the received symbol. Here we only need to watch out for the number of symbols in the modulation scheme. For QPSK we have a k = 4, 16-QAM a k = 16 and 64-QAM a k = 64.

3.2.1. Monte-Carlo-Simulation

Monte Carlo Simulation is widely used in stochastics to get solutions for random experiments. It is applied to solve analytical unsolvable problems numerically. MC is based upon the law of large numbers, which says that a large number of performing the same random experiment will lead the average of the results close to the expected value. We take this as a base to get reliable results. The Monte Carlo simulations will be used for two calculations, once already used above for calculating the differential entropy and later once to calculate a theoretical Rayleigh fading curve out of the AWGN channel.

3.2.2. Implementation in MATLAB

We now implement all the mentioned Equation (3.8) and (3.9) in MATLAB and plot the results. The code has to take into consideration the modulation schemes used, the range of calculation (SNR) and the sample size N. The code runs through the SNR range, here ranging from -10 dB to 30 dB in step sizes of 0.5 dB. The sample size N also has to be large enough to apply the Monte-Carlo simulation reliably. In our simulation N has to be higher than 10000 samples to receive reliable results. First a random bit stream, functioning as the data, is initialized. The bit stream is passed through a modulator which assigns the corresponding symbol. We scale the created constellation point with the SNR value. After passing $\underline{X}$ through the complex AWGN channel the resulting symbols $\underline{Y}$ and $\underline{X}$ are put into equation Equation (3.8) and (3.9). Done for every stepsize a resulting plot for

the capacity over SNR is created.

3.3. Results

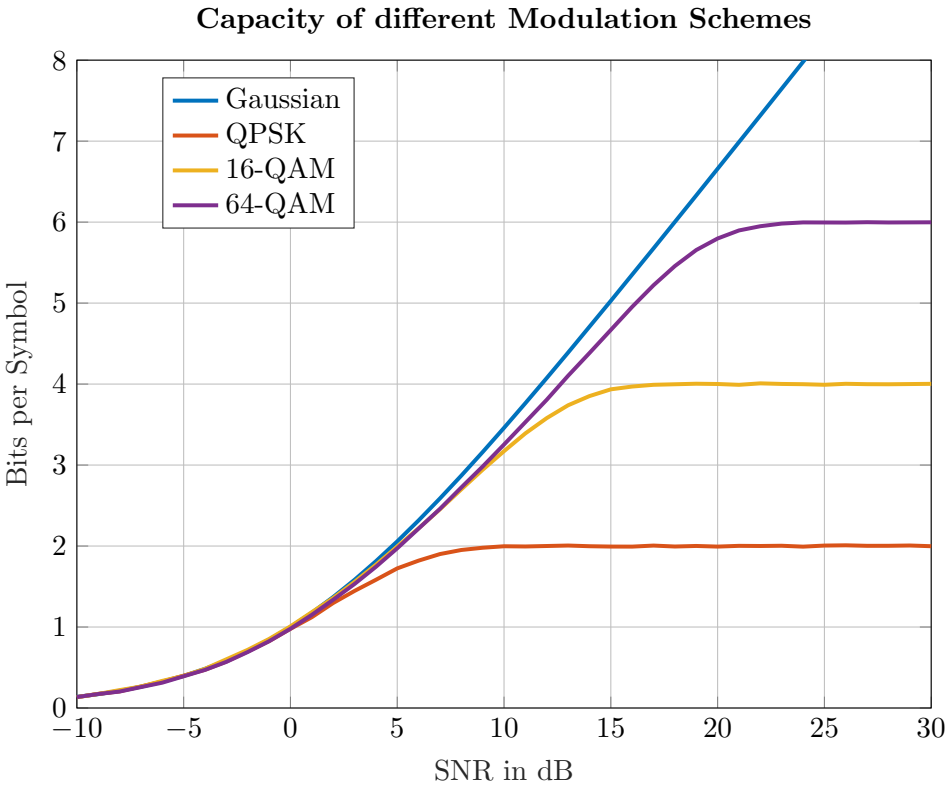

Figure 3.1.: Capacity plot for general AWGN-channel, QPSK, 16-QAM and 64-QAM

After all the Monte-Carlo-Simulation (MC) are done in MATLAB for all the modulation schemes the results are presented in Figure 3.1. The plot shows the capacity for a simple AWGN channel and the three modulation schemes mentioned in Chapter (2.3). We plot the resulting capacity calculated over the corresponding SNR value. It can be seen that for all three modulation schemes that for higher signal-to-noise ratio (SNR) they approach the desired maximum number of bits per symbol. Also the Gaussian channel clearly outperforms the modulated channels, especially after 0 dB SNR. AAs already discussed before the Gaussian capacity is the upper bound with no modulation exceeding it the following results and plot can confirm the validity of the simulation.

4. Frame Error Rate for AWGN Channel

This section will further built upon the topics discussed in the previous chapters. We will now build a communication chain using the blocks discussed in chapter (2). After the transmission the frame error rate (FER) will be determined. The FER is the estimated rate of faulty transmissions in one whole simulation. We will be sending frames of code words each consisting of 256 up to 2048 bits. After comparison between the sent code word and the decoded code word at the receiver we determine a frame error. If the decoded codeword has any wrong bit the whole frame will be marked as a faulty frame. This will be done for a certain amount of frames.

4.1. LDPC and the Coded Modulation Library

Already explained in Chapter 1 the whole transmission will be done with the coding method of LDPC. For the coding and decoding we will be using the Coded Modulation Library. This library and the functions used in this simulation will be further explained now.
The Iterative Solutions Coded Modulation Library (ISCML) is an open source toolbox for simulating capacity approaching codes in Matlab. (!cite!) The toolbox supports many different standard linear block codes and turbo codes. With many of the complex and computational heavy codes implemented in C and ported back to MATLAB as so called C-mex functions. (!cite!)
For this thesis a further look will be taken at the WiMax LDPC code. The coder function will create the parity-check-matrix **H** with a given code word length n and rate r. The code word which will be sent will be created like this:

$$\boldsymbol{H} * \boldsymbol{a}^{\boldsymbol{T}} = \mathbf{0}, \tag{4.1}$$

with a being the code word transmitted. Further noted a consists of the relevant data a_d, which is known, and the unknown check nodes a_r.

$$\boldsymbol{a_r} = (\boldsymbol{H_k})^{-\mathbf{1}} * \boldsymbol{H_l} * \boldsymbol{a_n} \tag{4.2}$$

The decoding will also be done by the Coded Modulation Library (CML) which again uses the parity-check matrix **H**. The received code word has to fulfill this condition:

$$\boldsymbol{H} * \boldsymbol{b^T} = \mathbf{0}, \tag{4.3}$$

with b^T being the received code word. This will be checked with typical graph solving algorithms. For LDPC the commonly used algorithm is the sum-product algorithm. (explain? a lot of computation and explaining...) With the CML the first and last block of the full communication chain (Figure 2.1) is implemented.

4.2. Demapping after AWGN

Another big part of a functioning communication chain is the estimation of the code word from the received symbol stream $\underline{Y}$, which passed the channel experiencing various kind of noises and fadings. There are two main forms a restoring the code word, namely hard-decision demapping and soft-decision demapping.

4.2.1. Hard-Decision Demapping vs. Soft-Decision Demapping

We will now discuss the benefits between hard-decision and soft-decision demapping. Hard-decision demapping makes a decision based on the decision boundary of the received symbol. While soft demapping will take into consideration all symbol constellations in the modulation scheme. It is proven that soft demapping will achieve better demapping results while hard demapping is not as complex as soft demapping. (!!cite!!)In our case we do not mind a complex system which takes more time but are more focused on achieving the maximum rate of successful transmissions.

4.2.2. Log-Likelihood Ratio

A soft demapper will now be implemented in this system. The soft demapper will result in turning the symbols in the corresponding bit block.

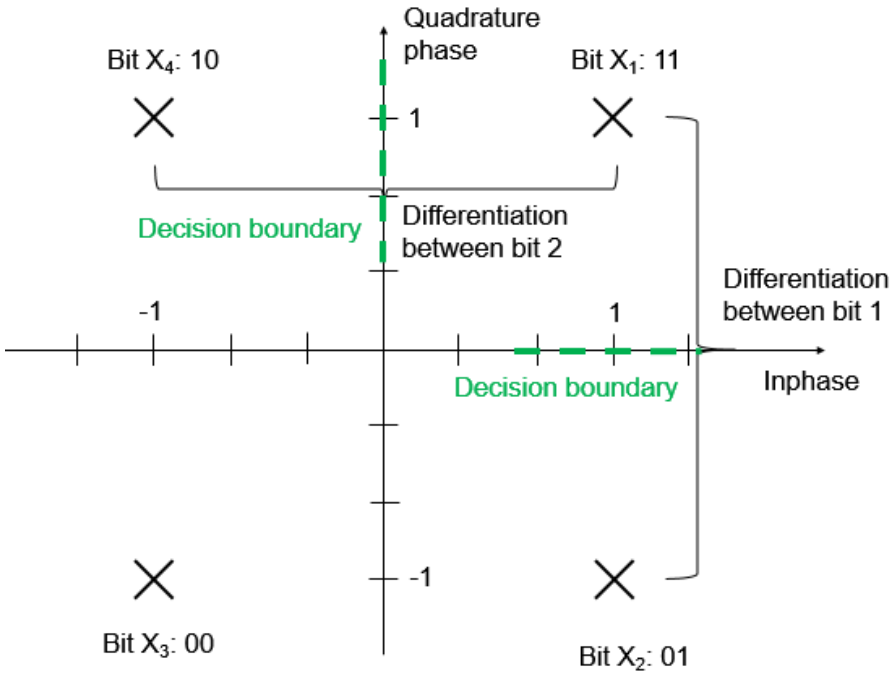

Figure 4.1.: PDF $p_N(N)$ of the number N of times that the head side is up.

As seen in the figure above we have a QPSK modulated codeword. Symbols $\underline{\mathbf{Y}}$ received can be located anywhere on the I/Q-plane distorted by AWGN. We will now assume a single symbol Y received at the demapper. With QPSK consisting of two bit blocks $[B_1 B_2]$ first a differentiation for the first bit is done.

$$L^n = log\frac{P(B_1 = 0|Y)}{P(B_1 = 0|Y)} \tag{4.4}$$

With Baye's rule:

$$P(B_1 = 0|Y) = \frac{P(Y|B_1 = 0)}{p(Y)} * P(Y = 0), \tag{4.5}$$

the equation simplifies to

$$L^n = log\frac{P(Y|B_1 = 0)}{P(Y|B_1 = 1)}, \tag{4.6}$$

with $P(Y = 0) = P(Y = 1) = 0.5$. Getting back to Figure 4.1 it can be determined that X_1 and X_4 have $B_1 = 1$ while X_2 and X_3 result in $B_1 = 0$.

$$L^n = log\frac{P(Y|X_2) + P(Y|X_3)}{P(Y|X_1) + P(Y|X_4)} \tag{4.7}$$

With Equation (2.4) the log likelihood for bit B_1 can now be calculated. The corresponding bit B_2 will also be determined like this. In the end a code word is received as log likelihood ratios.

4.3. FER

The FER can now be determined with the help of the two previous sections. By dividing the number of faulty frames from the total number of frames we get the FER. It should be noted that not every FER calculated is a reliable result for our simulation. For a whole simulation run a certain amount of faulty frames is needed, usually at least 50 faulty frames need to be detected. It can be seen like this: A simulation run for 100 frames with 1 faulty frame does not give a confident result of a FER of 0.01. While a simulation ran for 10000 frames with 100 faulty frames will be seen as a more reliable result of a FER of 0.01.
With the proposition above for a FER of 10^{-4} we would need to run a simulation with 10^6 frames. Now the problem of simulation time length arises. If lower FER needs to be calculated the number of frames will rise. Also while maybe feasible for short SNR-ranges some calculations will need longer SNR-ranges, which becomes a problem in the further chapters for fading channels. Both combined will make the simulation run rather long.
Two methods to reduce the simulation time are now implemented: The first one being a premature break of the simulation after reaching 100 faulty frames and dividing by the number of iterations ran. Even if running the whole simulation resulting in more precise FER, 100 faulty frames are enough for plotting a reliable result. Another technique is to increase the step size of the SNR between simulations, which will allow us to keep the SNR range at the expense of plot resolution. This can be mitigated by interpolating the results, which means we numerically create more data samples to increase the plot resolution.

4.4. Simulation Results

All the above discussed methods are implemented in MATLAB. The simulation will be run for an SNR range of 0-10 SNR. Furthermore a FER of at least 10^{-3} should be calculated, which is a total of 10000 frames run. The following plot shows the FER plots for all three modulation schemes. Now with the FER calculated the capacity plots from chapter (3) can be used again for comparison. In this part the FER calculation are used by examining the interpolated data. Setting a threshold at 10^{-3} FER the corresponding SNR value is noted down. The value is then plotted into the capacity plot. It has to be taken into account the rate of LDPC coding. The rate defines the amount of relevant data in a whole frame/code word. That means for a rate of 1/2 the transmission of relevant data is halved. For QPSK with a maximum of 2 bits per symbols and a rate of 1/2 a information value of only 1 bit per symbol can be achieved.

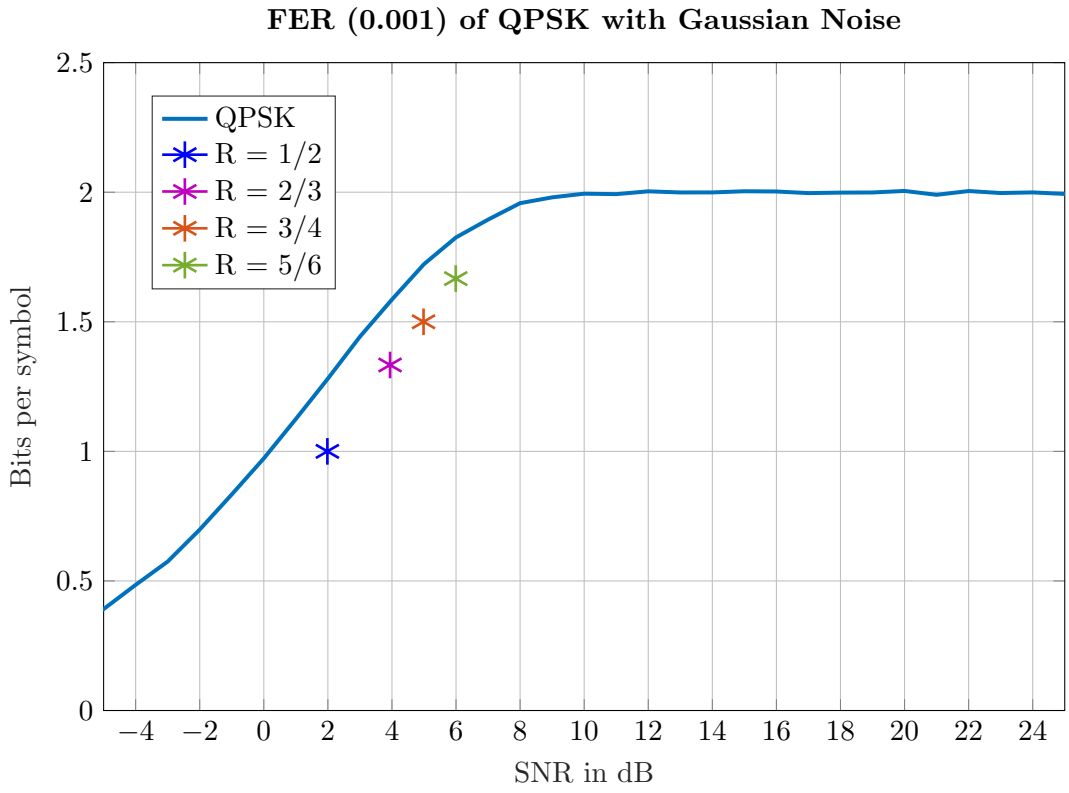

Figure 4.2.: Capacity to FER comparison for QPSK

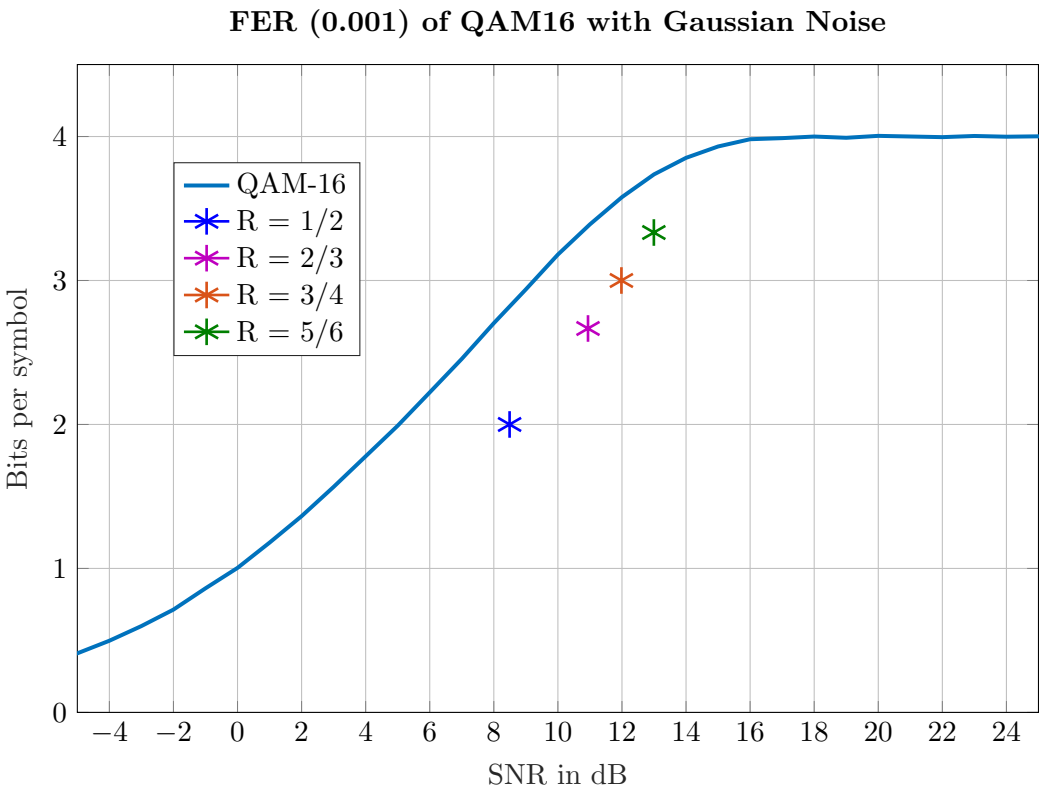

Figure 4.3.: Capacity to FER comparison for 16-QAM

The first Figure 4.2 shows the QPSK capacity plot from Figure 3.1. The capacity plot is needed to give reference for the FER points. For any FER point found it needs to be close to the capacity plot but not surpass or even touch the plot. It can be seen that for all four rates simulated the points are not surpassing the SNR, and therefore the efficiency, of the initial capacity plot.
For the next two figures, Figure 4.3 and Figure 4.4, the same procedure has been done. For all four available rates in WiMax coding the corresponding SNR value for the FER of 10^{-3} is plotted. It can be observed that also for these plots every rate is below the before calculated capacity plot. Transmission to achieve our desired FER will lead to an increase of SNR which also means that the overall transmission power need to increased. In Figure 4.2 to reach the FER for the rate of 1/2 from the capacity plot an increase of about 2 SNR is needed. This corresponds to a increase of the factor 1.6 in terms of power needed to reach the FER of 0.001. The same observation done for both 16-QAM and 64-QAM will result in deviating results. For 16-QAM an increase of about 3 dB is needed, which corresponds to an increase of power of the factor 2. 64-QAM on the other hand needs about 5 dB, which results into a overall increase of power consumption of the

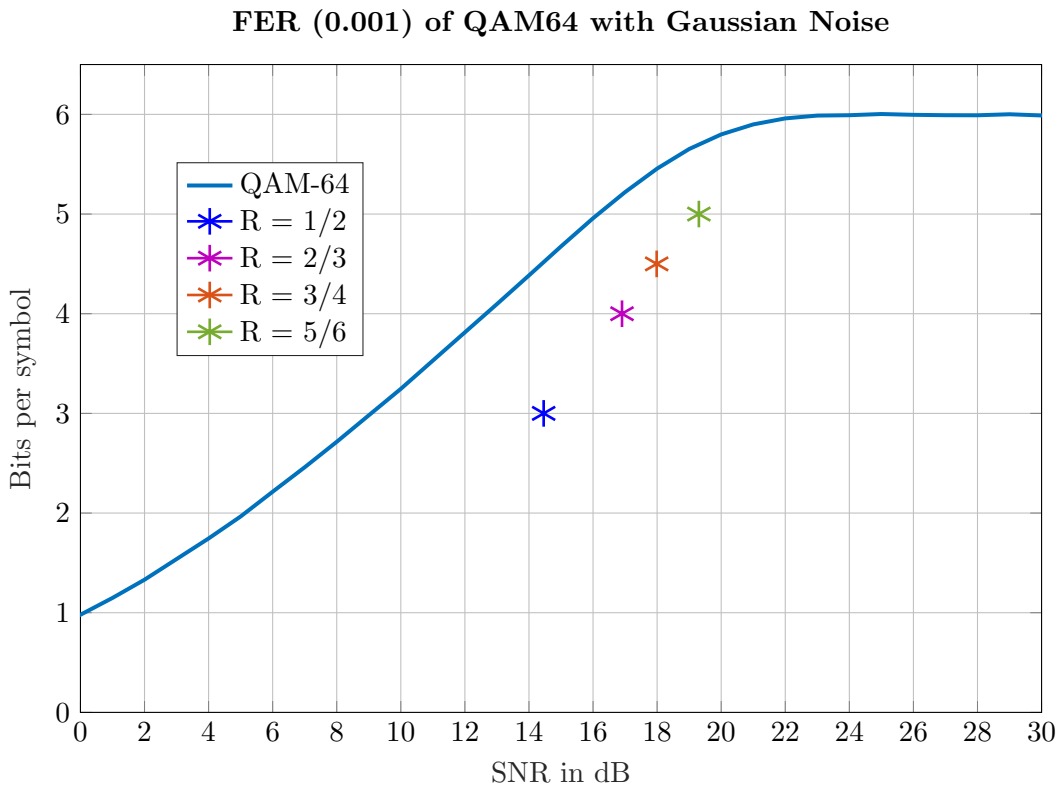

Figure 4.4.: Capacity to FER comparison for 64-QAM

factor 3.

Another observation from all three plots is the decrease in SNR needed for higher rates. While not very significant for QPSK where the decrease for the rate 1/2 to 5/6 is not very noticeable, the decrease in the other two plots is remarkable. For 16-QAM we save about 1 dB and for 64-QAM the save is 2 dB. In general it is to be expected that for a real communication system simulation that it is always performing worse than the capacity from a simple channel simulation. With the comparison between the FER points and the previous calculated capacity plots the simulation for a working transmitter receiver is confirmed and can be used for further simulations with different channel settings.

5. Capacity in a Rayleigh Channel

We will now discuss the above implemented simulation in AWGN with the addition of Rayleigh fading. There are many different fading processes that can be considered for simulation. In this thesis we will look at the so called block fading channel. In a block fading channel the fading coefficient H is constant over the block length $\mathbf{T}$. After every block the fading coefficient will change to a new independent value based on the distribution used. Block fading also includes that the fading is slow, which means that the doppler spread is low and the frequency does not vary much for a symbol duration. Slow fading is given when looking at block fading channels. Another important fading, the fast fading, occurs for multipath resulting in constructive and destructive interference patterns. Fast fading varies a lot and can change rapidly within one symbol duration. This means that we will not be using fast fading for this simulation. The type of fading used is called Rayleigh fading, also mentionend before in chapter (2.4.2). For the whole block fading simulation two different scenarios will be considered:
First of all for both scenarios "Channel distribution information" (CDI) will be applied, which means that both for the transmitter and the receiver the distribution of the fading coefficient is known. For the first scenario, additionally to CDI, the knowledge of the fading coefficient power will be given to the receiver. This scenario is also known as "Receiver CSI", with CSI standing for "channel side information".
In the second scenario the information of the fading coefficient power will be unknown, which means a method is needed to try to estimate the coefficient as accurate as possible.

5.1. Fading Channel

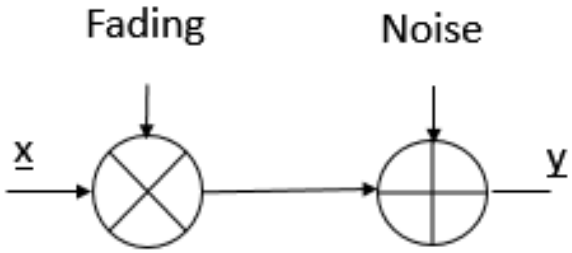

Figure 5.1.: Power spectral density for a AWGN channel

In comparison to the AWGN channel where only additive noise is added to the transmitted information signal. In the Rayleigh fading channel before addition of noise to the signal is done, the signal is scaled with the fading coefficient. Also mentioned in chapter (2.4.2) and the corresponding equation (2.5). As seen in Figure 5.2 with various fading coefficients the overall power of the signal can increase or decrease, which also results in a bigger/lesser interference of AWGN noise. Still it is important to know, while higher "power" is beneficial for the error probability in the system it is not needed to maintain stable information rate. At the same time a decrease in "power" will make the system suffer a loss in information. So in the end it is from utmost importance to try and reduce the fading from the received signal $\underline{Y}$.

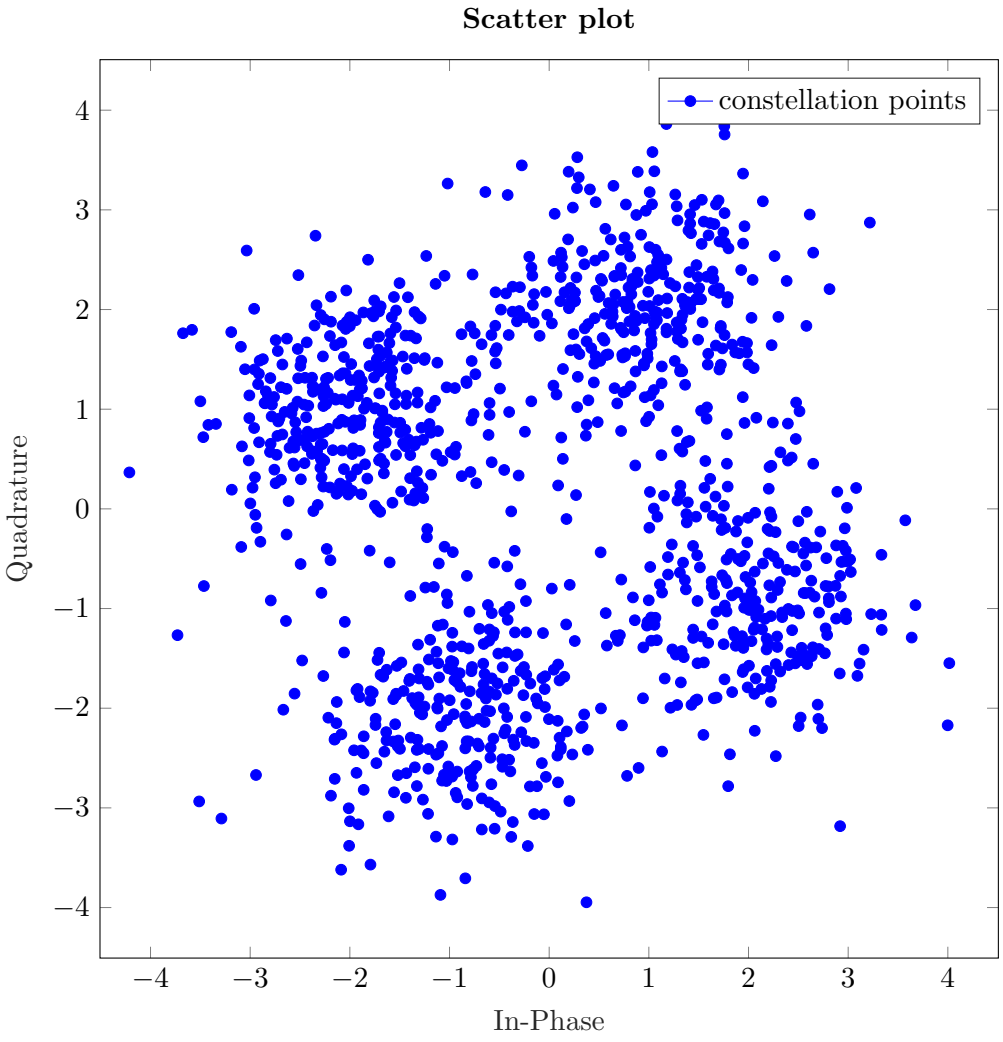

Figure 5.2.: Scatterplot for constellation points with Rayleigh fading in I/Q-plane.

5.2. Receiver CSI

We will now discuss recovering the signal with perfect channel knowledge.

$$\underline{Y} = H * \underline{X} + \underline{N}, \tag{5.1}$$

With the knowledge of the fading coefficient a simple division of the equation will solve the problem.

$$\hat{\underline{Y}} = \underline{X} + \hat{\underline{N}}, \tag{5.2}$$

with $\hat{\underline{Y}}$ being the new estimation of the received code word and $\hat{\underline{N}}$ the division of the noise with the fading coefficient. Although the fading has been removed from the initial sent code word the restored code word $\hat{\underline{Y}}$ has still to be considered a fading channel because of $\hat{\underline{N}}$. It is expected to have a decrease in performance in comparison to a normal AWGN channel.

5.3. Fading estimation with pilot symbol

In this section the scenario is taken into consideration that the receiver does not know the fading coefficient, but still has the information of fading block length. Now a method of restoring the code word $\underline{Y}$ has to be found.
One common and simple method used is the addition of pilot symbols into the codeword. To the code word additional pilot symbols will be added. In this simulation only one pilot symbol per block has been added.

$$\underline{X} = [X_T, X_1, ..., X_N] \tag{5.3}$$

The pilot symbol X_T has a set constant value both known at the transmitter and receiver side. With this knowledge an easy estimate can be given for the fading coefficient for each block.

$$Y_T = H * X_T + N \tag{5.4}$$

$$\hat{H} = \frac{Y_T}{X_T}, \tag{5.5}$$

being an estimate because of the unknown portion of noise. With an increase in transmission power an increase of accuracy in the estimation of H can be given. A recovery of the received signal $\underline{Y}$ with the estimate $\hat{H}$ will be done. It is to be expected, that this method will result in a worse performance than the recovery with the perfect channel knowledge.

5.4. Simulation Results

This section will discuss some cases simulated in this thesis. We will differentiate between different block sizes.

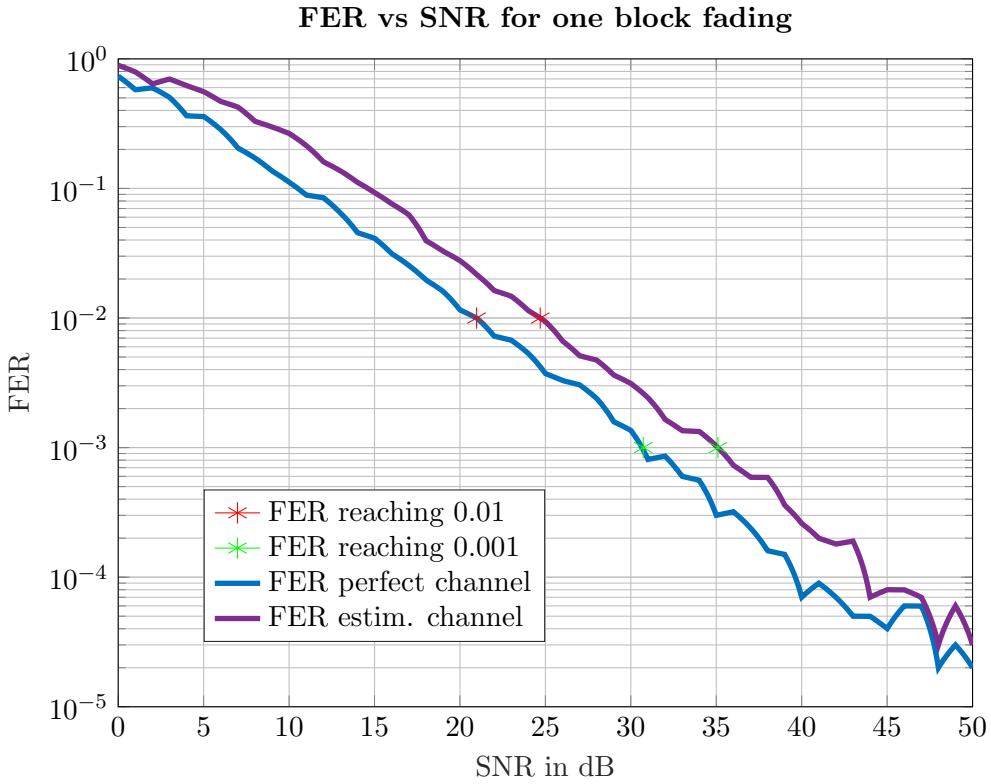

Figure 5.3.: Simulation for rayleigh channel with known and estimated fading coefficient

As seen above the simulation with perfect channel knowledge clearly outperforms the one with unknown fading coefficient. To be exact for both the FER of 10^{-2} and 10^{-3} a improvement of about 3.5 dB to 4 dB can be seen. This corresponds to more than the power consumption in the estimated channel to get the same performance than the perfect channel.

In the second Figure 5.4 different block lengths T are simulated for the channel with unknown fading coefficient. The block lengths here consists of the previous two plots and the new additional block lengths of two blocks and sixteen blocks per transmission. An observation can be given for low and high SNR behavior. For shorter block lengths, which means more blocks per transmission, the performance in low SNR is slightly worse while the performance in high SNR is slightly improved. For sixteen blocks per transmission this decline/improvement is not very noticeable.

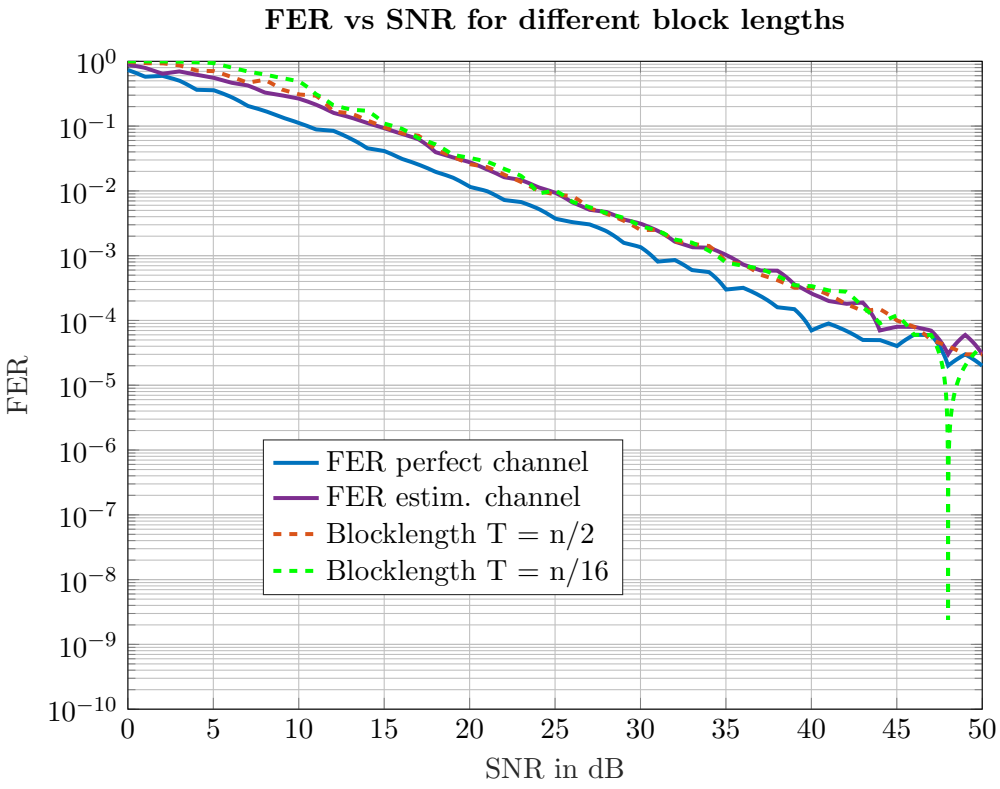

Figure 5.4.: Simulation for rayleigh channel with different blocklengths

In the last Figure 5.5 the extreme case of 1 symbol per block will be simulated. That means T equals to the number of transmission symbols. This kind of transmission from the view of viability is not feasible, because for every symbol a pilot symbol is added. With an addition for every symbol the whole transmission is slowed down by exactly half the rate, because overall twice the number of symbols need to be transmitted. But for this case the behavior for low and high SNR can be examined more precisely.
Here it is very clear that the newly simulated channel performs worse than the estimated channel for low SNR from 0 dB up to 16 dB, afterwards the channel outperforms the estimated channel and closely approaches the FER of the channel with perfect channel knowledge. It can be assumed that for low SNR the fading can be very strong, especially modulating every symbol independently it is to be expected that some of them will be modulated with very deep fading. The same independent single symbol fading can be an advantage for higher SNR. At the same time for higher SNR the occurrence of deep fading will reduce. Of course some cases of deep fading will still happen, but only affecting one single symbol every time, this can be easily recovered by the decoder. If deep fading occurs for longer block lengths it can be very obstructing even in higher SNR. This can

be mitigated with the single symbol per block or just small block length transmission.

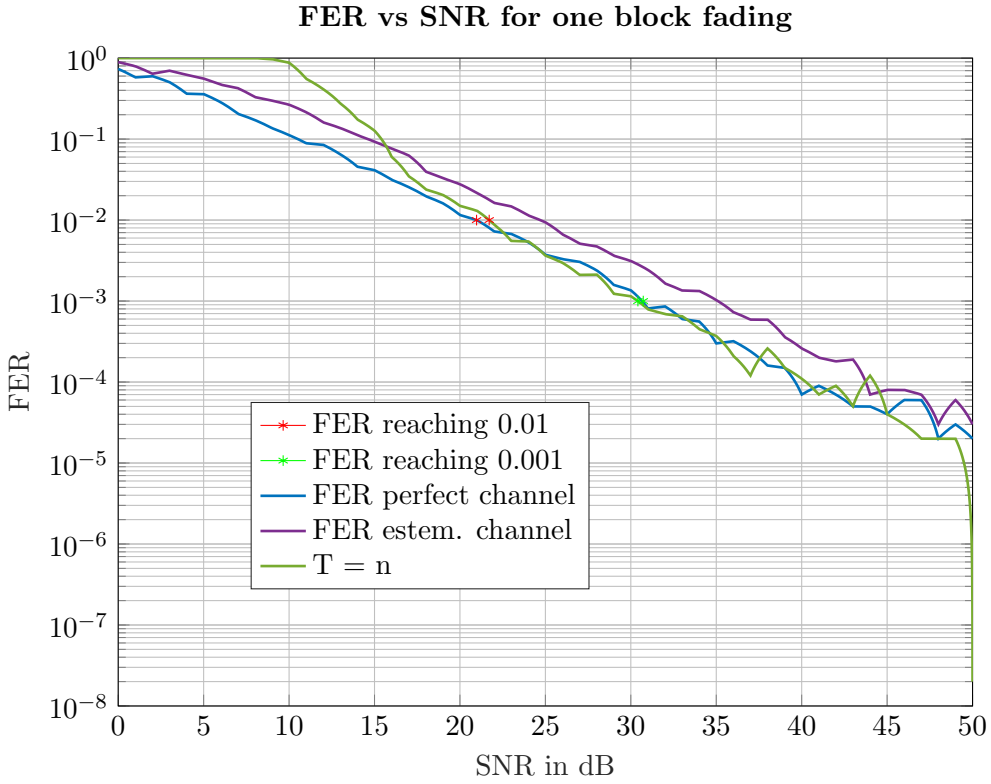

Figure 5.5.: Simulation for rayleigh channel with block length equaling to the number of symbols in each transmission

6. Further simulations to support the thesis

In this chapter we will discuss further simulations done to support the previous chapters. First of all a simulation to compare the FER simulated in chapter 5 will be initialized.

6.1. Simulated Rayleigh FER with AWGN channel

In this section a simulation based on the AWGN channel will be done to create a theoretical FER for a Rayleigh channel. This is done to have a reliable comparison for our simulation in Chapter 5. With the AWGN channel the reliability of the channel has already been proven with the capacity calculations from chapter 3. In chapter 4 the FER from the AWGN channel was in range of 0 dB up to 5 dB SNR. In this region a valid FER was given with the number of frames set. For this simulation first of all an AWGN channel will be simulated for the given range of 0 dB to 5 dB SNR. Then SNR from 0 dB to 50 dB SNR will be initialized. The SNR will be modulated with complex Gaussian noise to simulate the Rayleigh fading channel. For the now modulated SNR the corresponding FER can now be picked out. To get reliable results the MC will be applied again. For every step of SNR many independent fading coefficients will be created. The mean of all FER values will be taken to get the final data point plotted for the corresponding SNR value.

$$SNR_{ray} = SNR_{AWGN} * \mathbf{H} \tag{6.1}$$

$$FER_{ray} = FER_{AWGN}(SNR_{ray}) \tag{6.2}$$

In Figure 6.1 the FER for the AWGN channel is depicted. As mentioned above the valid range is only for 0 dB up to 5 dB, which will be a problem for higher SNR values. For higher SNR values an error floor must be initialized. The error floor is the lowest probability the FER can take. It is proven that every transmission will have a small probability of failure, no transmission will have 0 FER which would mean that a transmission can always be without any errors. In practical transmissions this is not achievable.

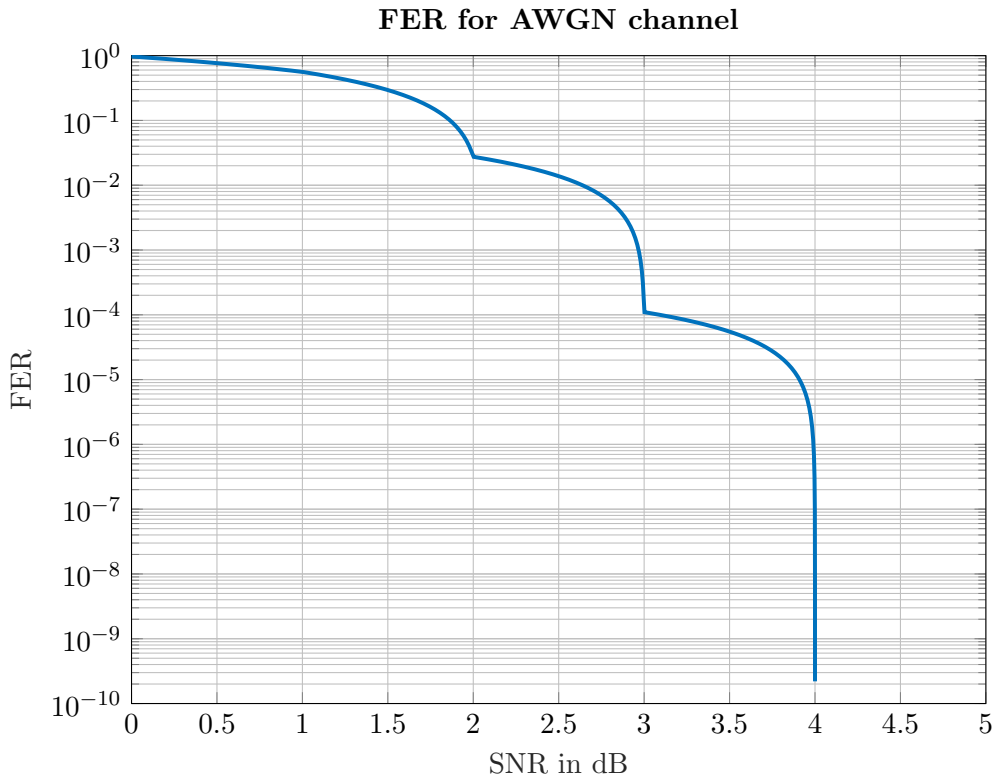

Figure 6.1.: FER for a simulated AWGN channel

In Figure 6.2 the FER of the AWGN channel is compared to the simulated FER of the rayleigh channel with error floors of 0 and 10^{-6}. It can be observed that Rayleigh fading deteriorates the channel performace by a lot in comparison to the simple AWGN channel. Furthermore as seen in the graphic the value of the error floor also needs to be determined. There is a offset when simulating the FER for different error floors, with the 0 error floor achieving way better FER than the one with an error floor of 10^{-6}. Now comparing the simulated Rayleigh fading based on the proven AWGN channel with our rayleigh fading from the rayleigh channel a statement can be given if the rayleigh channel was run properly.

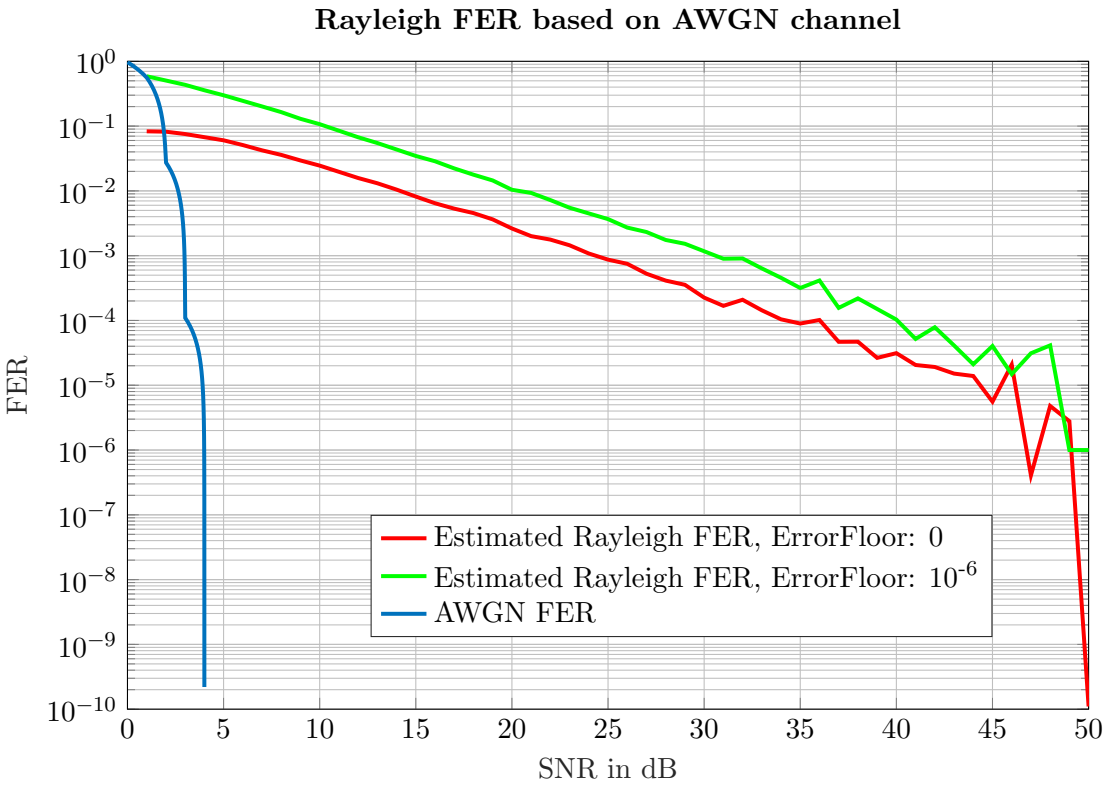

Figure 6.2.: Comparison between AWGN FER and Rayleigh FER

As seen in the last Figure 6.3 the simulated results based on the AWGN channel and the simulated rayleigh channel itself relate closely and behave the same way for different SNR values. With this section we proved that the simulated rayleigh channel is working as intended.

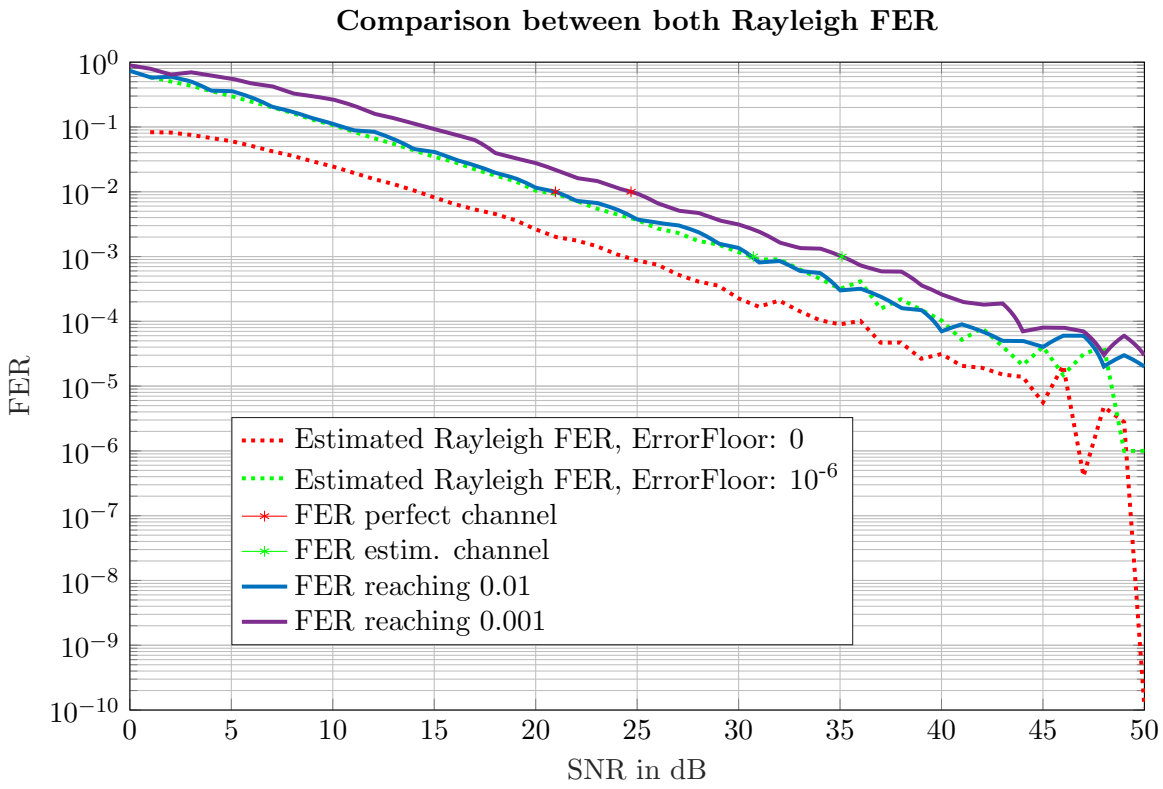

Figure 6.3.: Comparison of rayleigh FER based on AWGN channel and rayleigh channel simulation

6.2. Error floor calculation

As mentioned in chapter (6.1) the error floor should be determined to achieve proper results. In the previous simulation it was also determined that a deviation of a factor of 100 does not change the result of the plot by a lot. In our case it should be determined that the previous error floor of 10^{-6} is valid.
For determining the error floor the simulation of the AWGN channel is run. Important for this simulation is that the number of frames need to be changed. As mentioned in chapter (**??**) the validation of low FER needs high number frames. In our case we need a total number of 10^8 frames for every step of SNR. And the corresponding plot of the

SNR in dB	0	1	2	3	4	5
FER	0.9709	0.5618	0.0275	6.141e-05	3.6e-07	1e-08
Number of frame errors	100	100	100	100	36	1

Figure 6.4.: Data points from error plot simulation

data points. As seen in the figure and more importantly the data points our error floor of 10^{-6} can be confirmed. As mentioned before a minimum number of frame errors are needed to confirm a FER. While 36 frame errors are not the optimal number of errors it is still enough to validate an error floor of 10^{-6}.

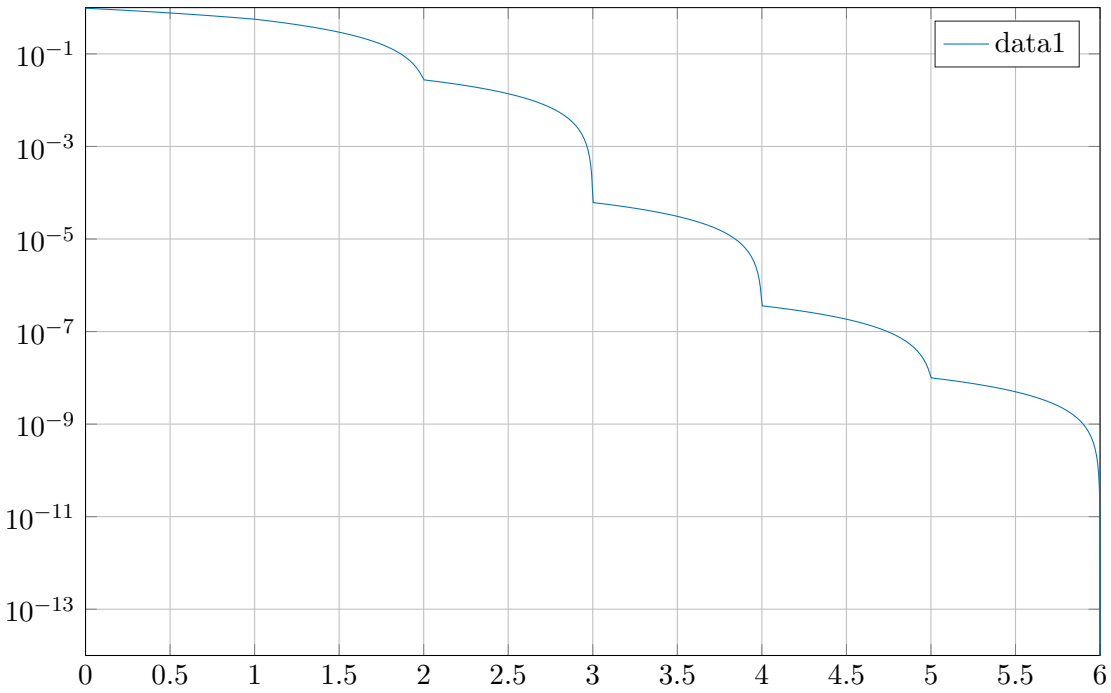

Figure 6.5.: Plot of error floor calculation

7. Summary

7.1. AWGN vs. Rayleigh Comparison

In this section a short summary between the two simulated channel is given. We will compare the methods and efficiency of both channels and relate it to real world applications.

Part I.

title

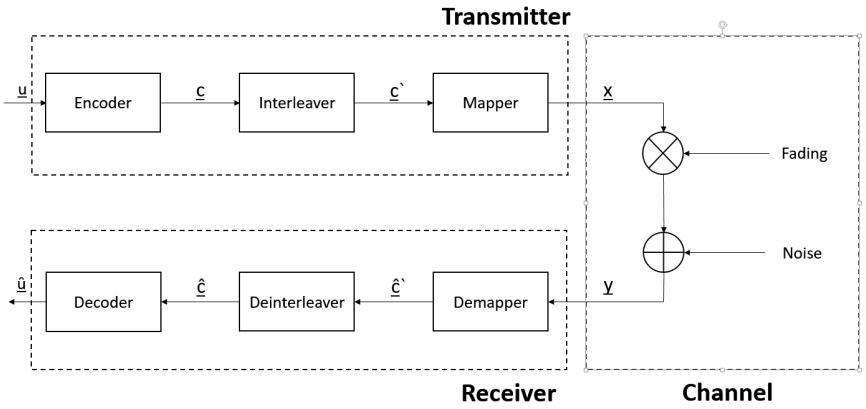

Figure 7.1.: PDF $p_N(N)$ of the number N of times that the head side is up.

Bibliography

[1] A. Goldsmith, *Wireless Communications*, 1st ed. New York: Cambridge University Press, 2008.

[2] J. G. Proakis and M. Salehi, *Fundamentals of Communication Systems*, 1st ed. Prentice Hall, 2004.

[3] B. Hassibi and B. M. Hochwald, "How much training is needed in multiple-antenna wireless links?" *IEEE Transactions on Information Theory*, vol. 49, no. 4, April 2003.

[4] A. M. Albert Guillén i Fàbregas and G. Caire, "Bit-interleaved coded modulation," *Foundations and Trends® in Communications and Information Theory*, vol. 5, 2008.

[5] G. Kramer, "Nachrichtentechnik 2," Manuskript zur Vorlesung, Lehrstuhl für Nachrichtentechnik, Technische Universität München, 2008.

[6] I. Solutions. (2007) The coded modulation library. [Online]. Available: http://www.iterativesolutions.com/Matlab.htm

[7] P. D.-I. S. ten Brink. Soft demapping. University of Stuttgart, Institute of Telecommunications. [Online]. Available: http://webdemo.inue.uni-stuttgart.de/webdemos/02_lectures/communication_3/soft_demapping/